Bioelectrochemistry 166 (2025) 109013

Contents lists available at ScienceDirect

Bioelectrochemistry

journal homepage: www.journals.elsevier.com/bioelectrochemistry

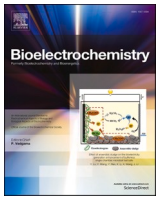

Electrochemical and bioelectrochemical ammonium recovery from N-loaded streams using a hydrophobic membrane☆

Zainab Ul[a], Mariella Belén Galeano[a], Mira Sulonen[a], Mireia Baeza[b], Juan Antonio Baeza[a,*], Albert Guisasola[a]

[a] GENOCOV, Departament d'Enginyeria Química, Biològica i Ambiental, Escola d'Enginyeria, Universitat Autònoma de Barcelona, 08193 Bellaterra (Cerdanyola del Vallès), Barcelona, Spain

[b] GENOCOV, Departament de Química, Facultat de Ciències, Universitat Autònoma de Barcelona, 08193 Bellaterra (Cerdanyola del Vallès), Spain

ARTICLE INFO

Keywords:
Ammonium recovery
Cation exchange membrane
Hydrophobic membrane
Microbial electrolysis cell
Ni foam
Stainless steel

ABSTRACT

Bioelectrochemical systems enable the recovery of ammonium from wastewater with low energy requirements and as a concentrated nitrogen-rich stream. This work aims to thoroughly investigate different cathodic electrode configurations and to optimize the operational conditions for active ammonium recovery from synthetic wastewater as concentrated ammonium sulphate. Different applied current intensities (50 mA, corresponding to 5 A m^{-2}, and 75 mA, corresponding to 7.5 A m^{-2}) and initial ammonium concentrations (between 0.3 and 3 g L^{-1} N-NH_4^+) were tested in an abiotic electrochemical system to understand the upper threshold of the used three-chamber configuration with hydrophobic membrane in terms of ammonium recovery rate (R_{rec}). With an external current of 75 mA, the highest value was 55 gN-NH_4^+ m^{-2} d^{-1} when removing 97 % from an initial ammonium concentration of 3 g L^{-1}. Bioelectrochemical ammonium removal/recovery was evaluated under different applied potentials (0.8, 1.0, 1.2, and 1.4 V) using two configurations: a Nickel-based gas diffusion electrode (GDE) and a configuration with the cathode (stainless steel or nickel foam) physically separated from the hydrophobic membrane. The highest removal rate (R_{rem}) (21 gN-NH_4^+ m^{-2} d^{-1}) was exhibited for stainless steel cathode at 1.4 V mainly due to its higher current density, which increased the cations migration. This higher R_{rem} also led to a higher R_{rec} (17 gN-NH_4^+ m^{-2} d^{-1}).

1. Introduction

In the last decade, much focus has been shifted from treating wastewater to channelling energy and nutrients contained in waste streams and reducing the burden and costs of wastewater treatment [1]. Bioelectrochemical systems (BESs) have been highlighted as an effective and sustainable technology for energy and nutrient recovery from wastewater [2]. However, BESs need to be further developed, optimized, and adequately integrated to be energy efficient and widely implemented in full-scale conditions.

Ammonium nitrogen in wastewater has emerged as an appealing compound from a resource recovery point of view. Industrially, ammonia is produced by nitrogen fixation (Haber-Bosch process) [3], which is highly energy-intensive and dependent on fossil fuels (ammonia production in 2020 reached 235 Mt. and accounted for 8.6 EJ, equivalent to 2 % of the total energy consumed globally) [4]. In a conventional wastewater treatment plant (WWTP), the entering ammonium is mostly transformed into nitrogen gas [5] through the nitrification + denitrification process in view of reducing the risk of eutrophication of receiving water bodies [6]. Thus, ammonium is removed but not recovered in spite of being a valuable product with multiple uses: a vast amount of nitrogen-based fertilizers are produced for agriculture [7] and ammonia has gained significant interest recently as a candidate vector for power generation [8]. The use of BES for ammonium recovery from wastewater holds promise as a suitable alternative in the circular economy framework.

BESs used for ammonium recovery can be divided into microbial fuel cells (MFCs) and microbial electrolysis cells (MECs) [9,10]. In MFCs, electricity is produced via spontaneous oxidation and reduction reactions [11]. In MECs, a small amount of external energy is applied to make the oxidation and reduction reactions thermodynamically feasible (i.e. hydrogen evolution reaction (HER) in the cathode) [12]. In both

☆ This article is part of a Special issue entitled: 'BES 2024' published in Bioelectrochemistry.

* Corresponding author.
E-mail address: JuanAntonio.Baeza@uab.cat (J.A. Baeza).

https://doi.org/10.1016/j.bioelechem.2025.109013
Received 28 September 2024; Received in revised form 21 May 2025; Accepted 30 May 2025
Available online 3 June 2025

BESs, anode-respiring bacteria oxidize organic matter to carbon dioxide and protons and use a solid anode as a terminal electron acceptor [13]. The electrons flow from the anode to the cathode through an external circuit. At the cathode, the electrons combine with an electron acceptor to form the target product. When recovering ammonium from streams containing organic matter, ammonium ions can be transported from the anodic chamber onto the cathodic chamber through a cation exchange membrane (CEM) via diffusion and/or current-driven migration [14]. Diffusion of ammonium ions is induced by the concentration gradient across the CEM, while the electric field drives the migration of ammonium ions to maintain the charge balance within the cell [15]. Therefore, ammonium ions can be concentrated in the cathode chamber or recovered with an additional recovery unit [9,16].

The ammonium ions have an acid-dissociation constant (p*K*a) of 9.25 (at 25 °C) [17]. Hence, once the solution pH exceeds 9.25, ammonium ions dissociate predominantly as free volatile ammonia (NH_3). In BES, cathodic reduction reactions such as hydrogen production can elevate the catholyte pH and drive the generation of dissolved ammonia, thus reducing the operating costs as the need for external alkali addition is avoided [16,18].

Once concentrated in the cathode, researchers have extensively studied two methods for bioelectrochemical ammonia recovery: 1) stripping the catholyte with air [3] and 2) hydrophobic membranes, such as in transmembrane chemisorption systems (TMCS), which are permeable to gases [19,20]. In both cases, ammonia can be recovered by successive absorption in an acid solution [3,21]. However, air stripping is often unfeasible since it incurs considerable energy input and creates a large volume of low-value off-gas [22–24]. Some studies using stripping as the recovery method reported energy consumption between 17 and 26 kWh per kg of ammonium removed [25,26]. Kuntke et al. achieved a recovery rate (R_{rec}) of 3.3 gN-NH_4^+ m^{-2} d^{-1} in a MFC [27], and Liu and co-workers reported a R_{rec} of 10 gN-NH_4^+ m^{-2} d^{-1} in a MEC using stripping [28].

Hydrophobic membranes allow less complex ammonia recovery and have a lower energy demand than the stripping method [29,30]. These membranes can be made of polymers like polypropylene (PP) [19], polyvinylidene fluoride (PVDF) [31], or polytetrafluoroethylene (PTFE) [21]. Dissolved ammonia gas in catholyte can pass through the pores of the hydrophobic membrane and react with an acidic solution placed on the other side [29]. Depending on the type of acid solution, ammonia could be harvested into ammonium salts such as NH_4NO_3 or $(NH_4)_2SO_4$, which can be used as liquid fertilizers. One of the most critical problems with using hydrophobic membranes is membrane fouling, but in most BESs, the catholyte in direct contact with these membranes is a clean alkaline solution that reduces the risk of fouling [21].

The hydrophobic membranes can also be used as carrier materials for a catalyst layer in constructing gas diffusion electrodes (GDEs). When employed in an air cathode [27], a R_{rec} of 3.29 gN-NH_4^+ m^{-2} d^{-1} was achieved at a current density of 0.50 A m^{-2}. Soon after, ammonium recovery using a gas-permeable hydrophobic tubular membrane was successfully demonstrated reaching R_{rec} of 19 gN-NH_4^+ m^{-2} d^{-1} [29]. The integration of ammonium recovery in a scaled-up MEC (0.5 m^2) using a gas-permeable membrane was also successfully achieved, showing the potential for a less complex and energy-efficient ammonium recovery step [16]. Cerillo et al. obtained a R_{rec} of 7 gN-NH_4^+ m^{-2} d^{-1} in a MEC (using carbon felt as anode and granular graphite as cathode) coupled to an ammonia recovery system based on a hydrophobic membrane. A much higher R_{rec} of 66 gN-NH_4^+ m^{-2} d^{-1} was achieved by Cerillo et al. in a MEC (carbon felt as anode and stainless steel as cathode) [32] fed with pig slurry (current density 1.40 A m^{-2}) [21]. More recently, Hou et al. obtained a R_{rec} of 36.2 gN-NH_4^+ m^{-2} d^{-1} at a current density of 25.5 A m^{-2} using a GDE [19]. These previous works demonstrated that hydrophobic membranes could be successfully employed in a MEC for ammonia recovery compared to the less energy efficient stripping method.

Using a GDE or a combination of a cathode and a hydrophobic membrane remains an open question. On the one hand, there is a lack of long-term operability of GDE for ammonia recovery and therefore needs further investigation. On the other hand, if the catholyte pH is not high enough, ammonium will predominantly convert to ammonia near the electrode surface, where pH is elevated due to the HER. This localized conversion can reduce system performance in the cathode + hydrophobic membrane set-up by increasing the distance between the electrode and the hydrophobic membrane.

The R_{rec} obtained in BESs have remained lower than those in abiotic electrochemical systems (ESs) with hydrophobic membranes, primarily due to the lower current densities in BESs [9,33]. For instance, an R_{rec} of 94 gN-NH_4^+ m^{-2} d^{-1} at a current density of 20 A m^{-2} was achieved by membrane stripping [30]. In another ES study, a R_{rec} of 1010 gN-NH_4^+ m^{-2} d^{-1} with a current density of 100 A m^{-2} using a hydrophobic membrane was obtained [34]. However, BESs allow ammonium recovery with lower energy demand due to part of the energy being recovered from the organic substances and the simultaneous treatment of the loaded water.

While an overall view of ammonia recovery using BESs is arising, some issues remain unresolved. Despite its essential role, the transport of ammonium ions through CEM is not fully comprehended. Since many cations are present in the anolyte, they compete with ammonium ions for transport across the CEM under current. Different studies reported that ammonium migration accounted for 30–90 % of the ionic flux in the BES depending on the initial ammonium in the anolyte [27,28]. As the ion transport depends significantly on the anodic and cathodic cation concentrations, understanding the relationship between the ammonium migration/diffusion through the CEM in biocompatible conditions that reflect wastewater is essential.

This study proposes a three-chamber MEC to assess ammonium recovery including a hydrophobic membrane system, providing new insights into relevant issues. First, the competition of ammonium transport with other cations was studied under biocompatible conditions in abiotic reactors. Bioelectrochemical ammonium recovery was then assessed using two different configurations: (i) the direct integration of the membrane electrode in the cathode chamber as a GDE and (ii) the use of hydrophobic membrane and cathode separately.

2. Material and methods

2.1. Experimental methodology

The selectivity of the ammonium transport from anolyte to catholyte through the CEM was first studied in abiotic experiments using a two-chamber setup. For these experiments, the chronopotentiometry operation mode was chosen between anode and cathode to avoid fluctuations in current density and, thus, in ion flux. Chronopotentiometry was performed using a programmable DC power source (LABPS3005DN, Velleman Group, Belgium). To determine the transfer rates and efficiencies of selected cations (NH_4^+, K^+ and Na^+), samples were taken from anolyte and catholyte before and after applying a constant current intensity of 50 mA for 24 h. An open-circuit experiment was also conducted to assess ammonium diffusion across the CEM. In these experiments, the system was left without power supply, and ammonium transport was driven solely by the concentration gradient between the anode and cathode. This experiment was carried out over a 24-h period with an initial ammonium concentration of 2 g L^{-1}.

Ammonium transport from anolyte to catholyte and to the recovery solution was then examined under constant current (50 mA, equivalent to a current density of 5 A m^{-2} or 75 mA, equivalent to a current density of 7.5 A m^{-2}) using a three-chamber setup. To calculate ammonium removal/recovery rates and efficiencies, samples were taken from anolyte, catholyte, and recovery solutions at the start and end of a 24 h period.

Finally, ammonium recovery was studied in three-chamber MECs, comparing two different configurations: a GDE and a configuration with

the Ni foam (NF) or stainless steel (SS) cathode physically separated from the hydrophobic membrane under different applied voltages (0.8 V, 1.0 V, 1.2 V, and 1.4 V) to determine the ammonium recovery, energy consumption and electrode stability with each material. A power source was used to apply voltage between the anode and cathode. The current intensity was monitored by measuring the voltage across a 10 Ω external resistor placed in the anodic connection. Voltage measurements were taken every 10 min using a 16-bit data acquisition card (Advantech PCI-1716) and controlled by AddControl software, developed by the GEN-OCOV research group in LabWindows CVI.

2.2. Reactors and materials

A set of three flat-plate BES (or MECs) reactors was built (Fig. S1 in the Supplementary Information). Each reactor had an anode chamber (0.4 L) including a carbon felt anode (Alfa Aesar, Germany, projected area per side 100 cm^2), a cathode chamber (0.2 L) separated from the anode chamber by a CEM (CMI-7000, Membranes Internationals, US) and one recovery chamber (0.2 L) separated from the cathode chamber by a GDE and/or a hydrophobic polyethylene (PE) membrane (DuPont, US). When a PE membrane was employed, the cathode used was either NF or SS. 3D printed spacers, made of PP, were placed in the anodic, cathodic, and recovery chambers to avoid deformation of the electrodes and membranes and promote mass transfer. The generated gas was collected with a gas bag connected to the top of the recovery chamber to prevent pressure buildup due to gas accumulation (primarily H_2). Gas production and its composition were not measured. A conceptual diagram illustrating ammonia recovery in MEC is depicted in Fig. 1.

2.2.1. Abiotic ammonium transport and recovery

In abiotic experiments, a Ni-PP based GDE was used as the cathode. The GDE consisted of a hydrophilic Ni top layer deposited on a hydrophobic PE support layer (0.22 um, Tisch scientific, North Bend, OH), which only allowed the passage of gases, such as ammonia/hydrogen. The detailed preparation route of the GDE can be found in the work of Hou et al. [19]. The GDEs were in direct contact with SS current collectors. The anolyte was a synthetic medium that contained the following per litre: 12.04 g L^{-1} Na_2HPO_4, 2.06 g L^{-1} KH_2PO_4, 0.2 g L^{-1} NH_4Cl, 4.0 mg L^{-1} $FeCl_2$, 6.0 mg L^{-1} Na_2S and 5 mL of a nutrient solution (g L^{-1}, 1 EDTA, 0.164 $CoCl_2{\cdot}6H_2O$, 0.228 $CaCl_2{\cdot}2H_2O$, 0.02 H_3BO_3, 0.04 $Na_2MoO_4{\cdot}2H_2O$, 0.002 Na_2SeO_3, 0.02 $Na_2WO_4{\cdot}2H_2O$, 0.04 $NiCl_2{\cdot}6H_2O$, 2.32 $MgCl_2$, 1.18 $MnCl_2{\cdot}4H_2O$, 0.1 $ZnCl_2$, 0.02 $CuSO_4{\cdot}5H_2O$ and 0.02 $AlK(SO_4)_2$).

Cation transport experiments were performed using two distinct catholyte solutions: (i) 4 g L^{-1} NaCl and (ii) a synthetic medium, identical in composition to the anolyte. The initial NH_4^+ concentration in the anolyte was varied in separate experiments, with concentrations of 0.5, 1, 1.5, and 2 gN-NH_4^+ L^{-1}. The anolyte composition remained consistent otherwise. The impact of different catholyte compositions on NH_4^+ transport was evaluated. The NaCl solution, with its simpler ionic composition, was chosen to better isolate the role of NH_4^+ migration. In contrast, the synthetic medium, containing additional cations, was tested to assess how the presence of other ions might influence the transport dynamics of NH_4^+. In a separate set of experiments focused on ammonium recovery, a broader range of initial NH_4^+ concentrations (0.3–3 gN-NH_4^+ L^{-1}) was tested to evaluate recovery efficiency under varying load conditions. The ammonium was recovered on the other side of the GDE as ammonium sulphate using 1 % sulphuric acid as the recovery solution.

2.2.2. Biotic ammonium recovery

In biotic experiments, three types of cathodes were tested, including NF (purity >99.99 %, 1.6 mm thickness, porosity ≥95 %; Recemat Ni4753.016); SS mesh (304, Feval filtros, Spain) and previously described GDE (projected area 100 cm^2). With NF and SS, titanium wire was used as the current collector.

The anode was inoculated with anaerobic sludge collected from a nearby wastewater treatment plant. The anolyte was a synthetic medium, recirculated at 15 mL min^{-1} through the anode chamber and an external reservoir (300 mL) using a peristaltic pump during the experimental period. Sodium acetate (1500–2000 mg L^{-1}) was added in the biotic tests to provide a carbon source for microbial activity. In contrast, no sodium acetate was added in the abiotic experiments, as the aim was to study how the cations in the synthetic medium behave without any microbial influence. Each experimental condition was tested in at least two independent batches to ensure reproducibility.

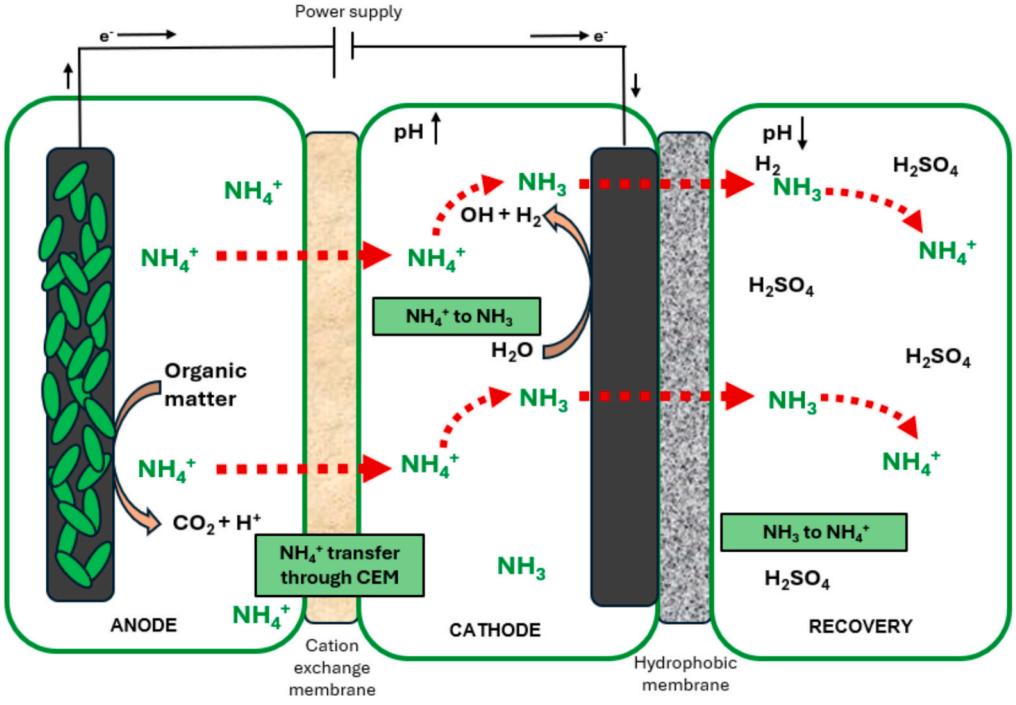

Fig. 1. Schematic representation of the MEC configuration used for ammonium recovery.

The catholyte (4 g L^{-1} sodium chloride) and recovery solutions (1 % sulphuric acid) were not recirculated. After every batch, the anolyte in the reservoir was replaced, acetate was added, and both the catholyte and the recovery solution were replenished. Electrochemical analysis of the SS material was carried out using cyclic voltammetry (CV) and chronoamperometry (CA). CV measurements were conducted between −0.1 V and + 1.1 V vs. Ag/AgCl at a scan rate of 20 mV s^{-1} in synthetic medium. CA was performed at a fixed potential of +0.3 V vs. Ag/AgCl for 30 min. All measurements were performed using a BioLogic potentiostat (BioLogic Science Instruments, France) in a standard three-electrode configuration, with the SS sheet as the working electrode, Ag/AgCl (3 M KCl) as the reference electrode, and a platinum sheet as the counter electrode.

2.3. Calculations

The current density was calculated based on the projected anode surface area. Ammonium removal efficiency (E_{rem}) was calculated with Eq. (1):

$$E_{rem}(\%) = \frac{N\text{-}NH_4^+ initial, anolyte - N\text{-}NH_4^+ final, anolyte}{N\text{-}NH_4^+ initial, anolyte} \cdot 100 \quad (1)$$

where $N\text{-}NH_4^+$ initial, anolyte and $N\text{-}NH_4^+$ final, anolyte are the initial and final concentrations of N-ammonium in the anolyte (g L^{-1}).

The ammonium recovery efficiency (E_{rec}) was calculated as the ratio between the final mass of ammonium in the recovery solution and the initial mass of ammonium in the anolyte (Eq. (2)).

$$E_{rec}\ (\%) = \frac{N\text{-}NH_4^+ final, recovery \cdot V_r}{N\text{-}NH_4^+ initial, anolyte \cdot V_a} \cdot 100 \quad (2)$$

where $N\text{-}NH_4^+$ final, recovery is the final concentration of N-ammonium in the recovery chamber (g L^{-1}), V_r is the recovery solution volume (L), and V_a is the anolyte volume (L).

The ammonium removal rate (R_{rem}) was calculated with Eq. (3)

$$R_{rem} = \frac{\left(N\text{-}NH_4^+ initial, anolyte - N\text{-}NH_4^+ final, anolyte\right) \cdot V_a}{A_{CEM} \cdot t} \quad (3)$$

where A_{CEM} is the CEM surface area (m^2), and t is time (d).

The ammonium recovery rate (R_{rec}) was calculated as Eq. (4).

$$R_{rec} = \frac{\left(N\text{-}NH_4^+ final, recovery - N\text{-}NH_4^+ initial, recovery\right) \cdot V_r}{A_{pp} \cdot t} \quad (4)$$

where A_{pp} is the membrane surface area (m^2), t is time (d), and $N\text{-}NH_4^+$ initial, recovery is the initial concentration in the recovery chamber (g L^{-1}).

The $N\text{-}NH_4^+$ load ratio L_N (−) was calculated as Eq. (5) [35].

$$L_N = \frac{i}{Q \cdot C_{anolyte,inflow,TAN} \cdot F} \quad (5)$$

where i is the applied current (A), Q is the anolyte inflow rate (m^3 s^{-1}), $C_{anolyte,inflow,TAN}$ is the molar concentration of total ammonium nitrogen (mol m^{-3}), and F is the Faraday constant (96,485 C mol^{-1}). In this study, the load ratio was calculated for an experimental period of 24 h.

Coulombic efficiency (CE) is the ratio between electron moles as current intensity to the total electron moles available from substrate oxidation (Eq. 6).

$$CE(\%) = \frac{\int_{t_0}^{t_F} I \cdot dt}{V_L \cdot b_s \cdot F \cdot \Delta C \cdot M_s^{-1}} \cdot 100 \quad (6)$$

where t_0 and t_F (s) are the initial and final times of a batch experiment, I (A) is current, V_L (L) is the volume of liquid in the reactor, b_s is the number of e^- transferred per mole of substrate, ΔC (g L^{-1}) is the difference between initial and final substrate concentration over the batch cycle, and M_s (g mol^{-1}) is the molecular weight of the substrate.

The transport number of ionic species i, is denoted as t_i, represents the fraction of the total charge flux carried by the ion i, relative to the total charge flux of all ions. This total charge flux is equivalent to the charge carried by the electrons through the external circuit. The transport number t_i is calculated as (Eq. 7):

$$t_i = VFz_i \frac{c_{i,o} - c_{i,t}}{\int_0^t I\, dt} \quad (7)$$

where z_i is the charge of species i, $c_{i,o}$ and $c_{i,t}$ are the concentrations of species i at times 0 and t, respectively, V is the volume of the compartment, and $\int_0^t I\, dt$ represents the total charge transferred through the external circuit during the experiment.

2.4. Chemical and optical analyses

Acetate concentrations were measured at the beginning and the end of each cycle with a gas chromatograph (Agilent Technologies 7820-A) employing a DB-FFAB column (30 m of length, 250 μm of internal diameter, and 0.25 μm of film thickness) and a flame ionization detector. The sample preparation procedure consisted of pipetting 800 μL of filtered samples (0.22 μm syringe filter) into a glass vial with 200 μL of preserving solution (used as an internal standard). The preserving solution was composed of 2 g of $HgCl_2$, 2 g of hexanoic acid, and 33.7 g of orthophosphoric acid in 1 L of deionized water.

Ammonium, potassium, and sodium concentrations were determined using a Dionex DX-120 ion chromatograph with an AS40 autosampler, an IonPac CS12A cation exchange column, a CSRS 300 suppressor (4 mm) (Thermo Fisher Scientific, USA) and 20 mM methane sulfonic acid as eluent at 1 mL min^{-1}.

The surface structure of each layer of GDE was visualized on scanning electron microscopy (SEM) using a Merlin Zeiss microscope operated at a 5 kV and with a dispersive energy X-ray (EDX) analysis system and Joel JSM 6010 (Joel, Ltd., Tokyo, Japan).

3. Results and discussion

The experimental results are categorized into two different parts. The first part, under abiotic conditions, aims at understanding the maximum ammonium R_{rec} in the existing set-up using current densities that are common in BES. The second part of the paper aims to compare these values with the long-term performance of several three-chamber MECs under different conditions.

3.1. Abiotic experiments

3.1.1. Cation transport through CEM under different conditions

The E_{rem} was quantified under different initial ammonium concentrations in the presence of common competing cations (Na^+ and K^+) and under a fixed applied current (50 mA) over a 24 h period. The aim of these experiments was to understand which cation transport dominated the charge transport across the CEM. For these experiments, the proton's contribution to current transport through CEM was not taken into account because the anolyte pH was neutral, and, under these conditions, their contribution is trivial [36]. Current density and the gradient of ammonium concentration between anode and cathode regulate the ammonium transport across the CEM [25,27,37]. Ammonium can also diffuse from the anode to the cathode with no applied potential due to an ammonium concentration gradient. As a standard base, diffusion accounted for a significant amount of ammonium removal (E_{rem} of 18 % in 24 h) in an open circuit with 2 g L^{-1} of initial ammonium.

Fig. 2 shows the net transport number of different cations for different initial ammonium ion concentrations and two catholyte solutions: a commonly used and high-conductivty solution concentration of 4 g L^{-1} NaCl (1.6 g Na^+ L^{-1}) and the mineral medium (containing 3.9 g

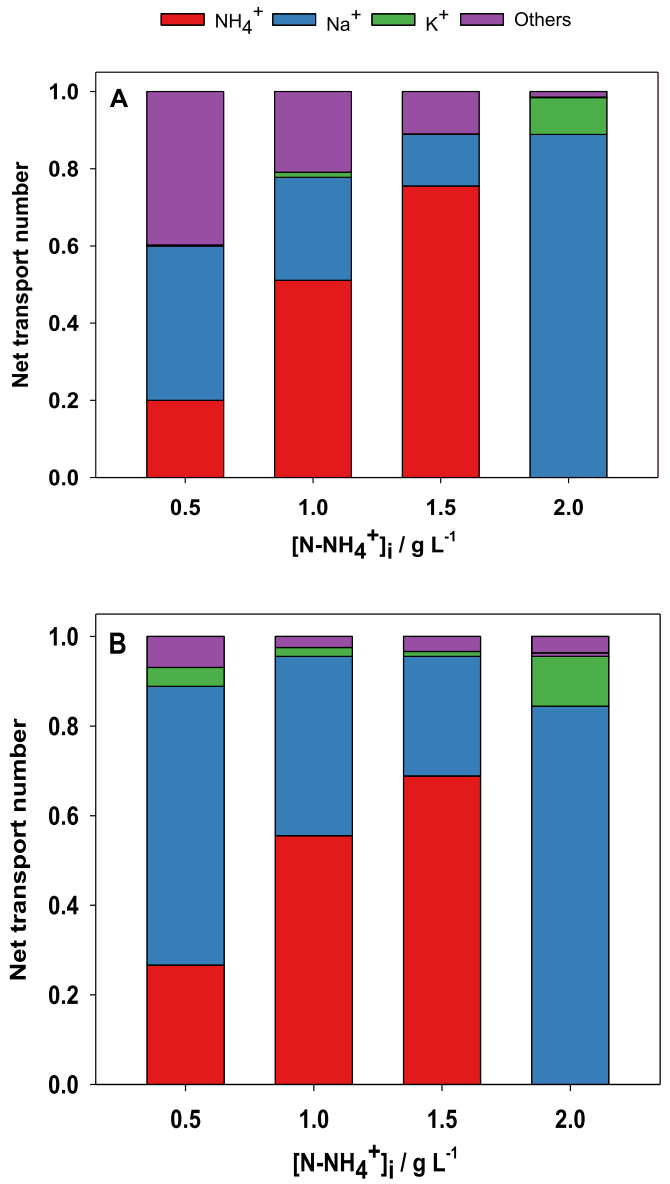

Fig. 2. Net transport numbers for different initial ammonium ion concentrations in the anolyte: a) with sodium chloride as catholyte and b) with mineral medium as catholyte.

L^{-1} Na^+ and 0.6 g L^{-1} K^+) [38]. For the first case (Fig. 2A), a higher initial ammonium ion concentration improved its transport as also observed in previous studies [14]. For an initial low ammonium concentration of 0.5 gN-NH_4^+ L^{-1}, only 20 % of the charge was carried by the migration of ammonium. Moreover, the absence of other cations (such as Mg^{2+}, K^+ or Ca^{2+}) in the catholyte also promoted their significant migration from the anolyte. Conversely, the transport of ammonium balanced 89 % of the charge at high initial ammonium concentrations (2 gN-NH_4^+ L^{-1}). Although transport numbers can vary with changes in cation molar fractions over time [39], in this study, net transport numbers were calculated based on ion concentrations measured after 24 h. These measurements established a baseline for ion transport and to evaluate the competition between cations over the course of the abiotic experiments. Other authors have also seen improvements in nitrogen flux (26 g_N m^{-2} d^{-1}) by using NaCl (0.1 g L^{-1}) as a catholyte as compared to using phosphate buffer (KH_2PO_4, 3 g L^{-1} and Na_2HPO_4, 6 g L^{-1}) as a catholyte [40]. As indicated in that study, which used a MFC configuration, the improvement was likely due to a decrease in internal resistance and an increased potential available for ion migration when NaCl is used.

When mineral medium was used as both the anolyte and catholyte (Fig. 2B), sodium accounted for 60 % of the charge transport at the lowest initial ammonium concentration. However, as the initial anodic ammonium concentration increased to 2 gN-NH_4^+ L^{-1}, ammonium became the dominant charge carrier, responsible for over 80 % of the total charge. In contrast, Yang et al., observed an increase in NH_4^+ recovery amount from 2.6 mmol to 3.05 mmol as the Na^+ concentration in the catholyte increased from 0.1 mmol L^{-1} to 30 mmol L^{-1} [41]. The authors attributed this improvement to Donnan dialysis, as the higher Na^+ concentration in the catholyte, without altering the concentration of other cations, facilitated NH_4^+ transport.

Potassium and sodium ions were the main cations competing with ammonium for transport across the CEM since they were present in higher concentrations than other cations in the anolyte. While the high permselectivity values of the CMI-7000 membrane for NH_4^+ (94 %), Na^+ (100 %), and K^+ (83.9 %) [42] provide insight into the membrane's preferential ion transport under equilibrium conditions, they do not directly reflect the transport numbers of the cations under operational conditions. In practice, cation transport through the membrane is governed not only by permselectivity but also by the relative concentrations and molar fractions of the competing ions in the solution. Therefore, even though the membrane shows a high intrinsic preference for Na^+ and NH_4^+, the effective transport of each ion is primarily dictated by their availability in the mixture. In this study, at lower NH_4^+ concentrations, sodium was the leading cation; however, at higher NH_4^+ concentrations, ammonium became the dominant cation. At the same time, potassium had little interference, even though it crossed the CEM. This suggests that improving ammonium transport through the CEM would require focusing on its concentration in the mixture, rather than relying solely on the membrane's permselectivity.

3.1.2. *Assessment of ammonium recovery under abiotic conditions*

Abiotic ammonium recovery was tested in the three-chamber setup and under two applied currents (50 and 75 mA) to be within the range of realistic intensities that can be usually obtained in a BES under biocompatible conditions. For these applied currents, a range of initial ammonium concentrations in the anolyte was tested (0.3–3 g L^{-1} N-NH_4^+). Fig. 3 illustrates the ammonium removed from the anolyte in 24 h for the two different applied intensities. As observed, a higher applied current provides more driving force for the migration of ammonium over CEM. With an applied intensity of 50 mA (Fig. 3A), the R_{rec} kept increasing when the initial ammonium concentration was increased stepwise from 0.3 gN-NH_4^+ L^{-1} to 2.3 gN-NH_4^+ L^{-1} but decreased with the highest tested initial concentration of 2.8 g L^{-1}. The highest R_{rec} obtained was 49 gN-NH_4^+ m^{-2} d^{-1} at an initial concentration of 2.3 gN-NH_4^+ L^{-1}. The limiting factor might be the cathodic pH, which, together with ammonium concentration, rules the flux of ammonia removal through the GDE (from the cathodic to the recovery chambers). High cathodic pH (leading to low ammonium and high ammonia concentration) is desired to enhance ammonium transport from the anode to the cathode through the CEM. In all cases, the cathodic pH was only between 8 and 9, which implies that less than a half of the ammonium nitrogen was in ammonia form. As a result, it was not effectively removed from the cathode via GDE, limiting the electromigration from the anolyte.

When the applied intensity was increased to 75 mA (equivalent to a current density of 7.5 A m^{-2}) (Fig. 3B), the increase in initial ammonium concentration led to higher rates. The maximum R_{rem} and R_{rec} values obtained with the highest tested initial concentration of 3 gN-NH_4^+ L^{-1} were 93 gN-NH_4^+ m^{-2} d^{-1} and 55 gN-NH_4^+ m^{-2} d^{-1}, respectively. The higher intensity was thus shown to improve the R_{rem} and R_{rec}, but the operation at high intensity was observed to cause damage to the GDE (results not shown), likely because of the high pressure built in the cathode chamber due to hydrogen formation. Therefore, higher current densities were not tested.

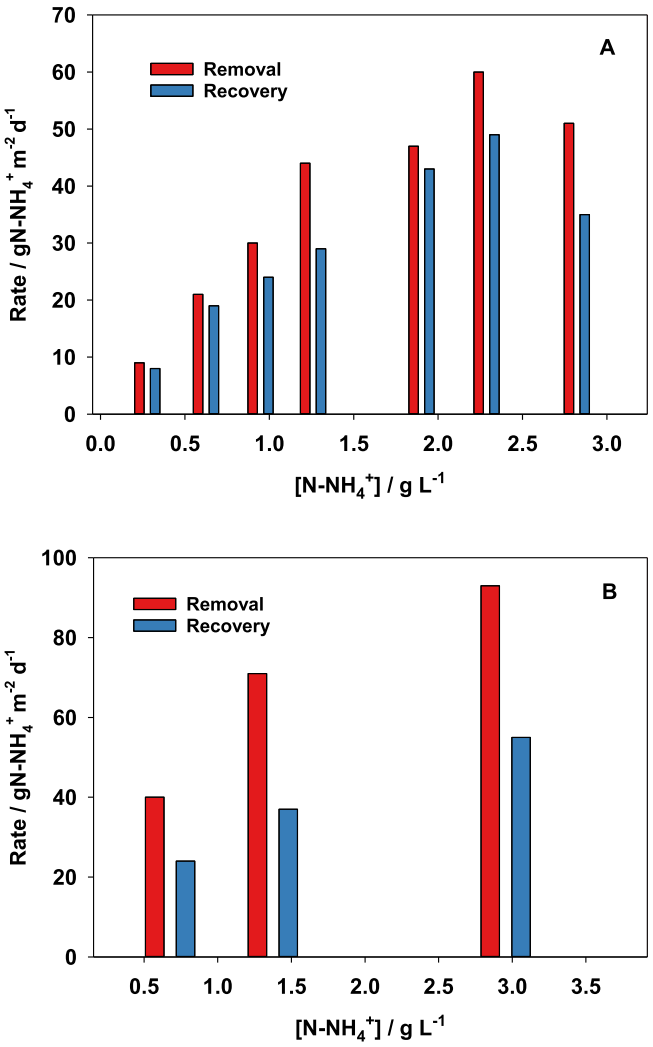

Fig. 3. Ammonium removal and recovery rates at different initial concentrations under an applied current of (A) 50 mA and (B) 75 mA.

Generally, it is not easy to find a good point of comparison between different ES studies for ammonium removal/recovery since different operation modes, current densities, different materials, and initial ammonium concentrations in the anolyte are used. Recently, it was proposed that the L_N is vital in determining ammonium recovery and energy input [43]. The L_N is the ratio between the current and ammonium loading rates. Fig. S2 shows the L_N for each of the experiments. This study's L_N were below 1 with an applied current of 50 mA (except for 0.5 gN-NH_4^+ L^{-1}), indicating that the applied current was insufficient to transport all ammonium within the experimental period of 24 h. With 75 mA of applied current, the L_N was higher but not above 1 for a given period of 24 h (except for 0.5 and 1 gN-NH_4^+ L^{-1}). For L_N lower than 1, it would have taken more than 24 h to remove all the ammonium from the anolyte.

Table S1 in the Supplementary Information presents a compilation of R_{rec}, current density, and L_N reported in previous studies working with recovery methods in ES. Our study yielded values within the range documented in the literature. However, the ES R_{rec} are much higher than we achieved, most likely because of our system's lower applied current density. The reasoning for using lower current density in our approach is to simulate realistic intensities achievable in a BES under biocompatible conditions. Higher current densities, particularly with non-adapted anodes, may lead to extreme anode potentials that could damage the biofilm. The ammonium flux through the hydrophobic membrane achieved by other authors is variable because it depends on the operational conditions. It ranges from 69 gN-NH_4^+ m^{-2} d^{-1}, using a hydrophobic membrane from synthetic wastewater [44], to 1010 gN-NH_4^+ m^{-2} d^{-1}, using a gas-permeable membrane with urine [34].

However, some operational changes could improve the system's performance; for instance, a continuous acid replacement could be a promising for the recovery solution to achieve a more stable ammonia flux through the hydrophobic membrane. The pH of the catholyte could be increased externally to make the ammonium conversion into ammonia more favourable. And lastly, the current density could be controlled in an ES to raise L_N and obtain a higher ammonium removal performance. Moreover, theoretically, almost half of the energy required to run an electrochemical cell for ammonia recovery could be recovered as hydrogen, a plus point for ammonia recovery in these systems [19].

3.2. Biotic experiments

We shifted from the chronopotentiometry method to a fixed applied voltage strategy between the anode and cathode for biotic experiments. In this approach, the anode potential for anode-respiring bacteria will change depending on several factors, such as substrate concentration, the applied voltage, and the type of bacteria present.

3.2.1. Ni-PP-based GDEs for ammonia recovery in BES

We started inoculating carbon felt anodes with anaerobic sludge and used a Ni-PP-based GDE as suggested in a previous work [19]. After 14 days of operation, we saw a decrease in the cell's performance. Due to the high pH gradient between the catholyte (pH > 8) and the recovery solution (pH < 2), the backflow of acidity was presumed to cause local changes in the pH on the surface of the GDE, leading to Ni dissolution (Fig. S3). Highly acidic recovery solution (~ 1 M H_2SO_4) and a high internal recirculation rate were observed to damage the GDE and led to the detachment of the electrodeposited Ni. The catholyte and anolyte solutions were observed to change colour to a light green, indicating the presence of Ni ions: Ni^{2+} was sporadically measured in the catholyte with values up to 700 mg L^{-1} Ni^{2+}. The Ni detachment directly decreased the cathodic performance. In addition, potential Ni transport through the anode presumably hindered anodic biomass growth.

3.2.2. Optical microscopy

Fig. 4 shows SEM images of the different layers of the Ni-PP-based GDE. The individual fibres were visibly identifiable in the pristine PP membrane (Fig. 4A). The multi-walled carbon nanotubes (MWCNT) entirely laminated the PP membrane, reducing the prominence of the threads and filling the gaps (Fig. 4B). Therefore, the membrane adhered to the MWCNT, indicating that the PVDF acted as a binding agent. The SEM image after the electrodeposition (Fig. 4C) indicates that Ni was successfully deposited on top of the MWCNT layer. However, the prepared GDE showed signs of deterioration, as seen after 14 days of operation (Fig. 4D). The MWCNT layer could also be visibly observed on the GDE, conforming to the detachment of Ni from the GDE. The backflow of the acid solution most likely caused the non-homogeneous distribution of a Ni layer on the GDE's surface.

EDX mapping (Fig. 4E and F) made it possible to track the stabilization of the Ni layer on top of the GDE. The EDX analysis primarily identified elemental Ni on the GDE's surface. Further analysis of the elemental composition showed significant chlorine, sodium, and potassium residues on the GDE after the operation. The Ni on the surface of the GDE and the chlorine from the catholyte solution most likely precipitated as Ni chloride. In contrast, chlorine was detected in a minor amount on GDE before the operation. The presence of other residues can be attributed to cation transport from the anolyte through the CEM. The formation of these precipitates is also favoured by the alkalinized catholyte solution, which promotes the formation of deposits [36].

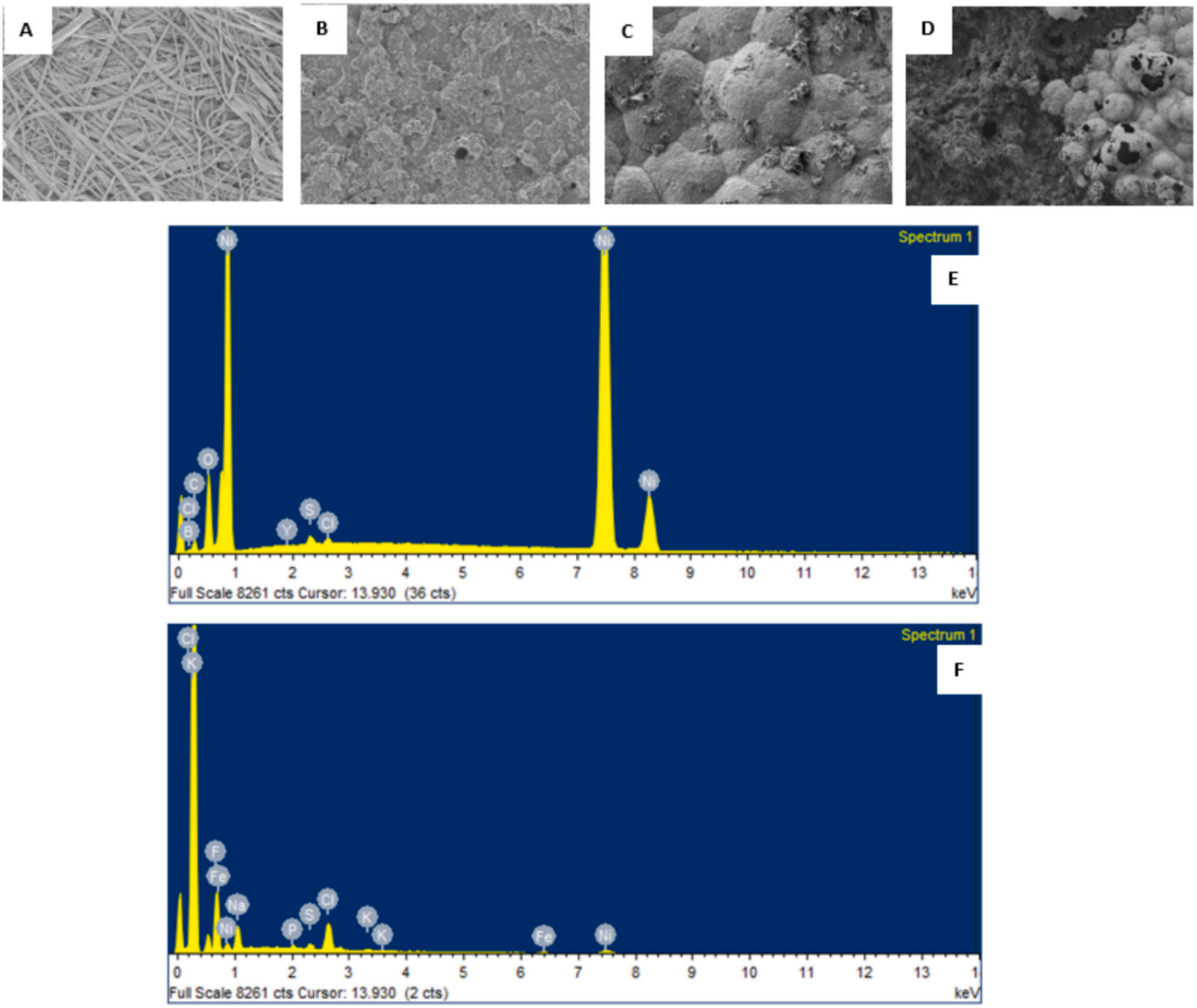

Fig. 4. Top: SEM images obtained at 1.00 kX magnification. A) PP membrane, B) manual airbrushing coating MWCNT, C) GDE before operation and D) GDE after the operation. Bottom: E) EDX results of the GDE before and F) after use.

3.2.3. Alternative cathode materials for ammonium recovery

To prevent the Ni from dissolving and to reach long-term ammonium recovery, we tested different membrane-cathode configurations:

1) reinforcing the hydrophobic effect of the GDE by adding an additional polyethylene (PE) hydrophobic layer between GDE and acid solution (Ni-PP-based GDE + PE),
2) separating the cathode from the hydrophobic membrane by using a NF electrode and a separated PP hydrophobic membrane (NF + PP).
3) replacing Ni from the cathode by using a SS electrode and a separated PP hydrophobic membrane (SS + PP).

Both SS and NF are known as excellent catalysts for hydrogen production in MECs [45,46] and their commercial availability, low cost properties, and long term stability have also been proven in literature [47,48].

Fig. 5 displays the current density of MECs using the three different methodologies described. As observed, the current density obtained with SS + PP was stable for almost two months and, therefore, could be a possible alternative for long-term operations. When it comes to NF as a cathode, it also showed a similar and stable current density as SS. Since ammonium migration depends on current, the increase in current led to an increase of the ammonium removal performance.

Adding a PE layer between the GDE prevented protons penetration from the recovery solution to the catholyte, which resulted in stable operation for 43 days. It also presented similar current densities than other cathode materials tested. The crystalline composition of the coated Ni layer on the GDE, with $Ni(OH)_2$, has been widely reported to enhance catalytic activities, thereby improving the HER during water splitting [49,50]. No significant Ni detachment was observed from the GDE after two months of operation probably due to protons being prevented from penetrate. Besides this, an advantage of using GDE for ammonia recovery is that it obviates hydroxide and ammonia accumulation, decreasing pH on the surface and, thus, the overpotential, and eventually improving current production [19].

In any case, the current densities obtained with biotic conditions were much lower than in abiotic systems. Regarding R_{rem} and R_{rec}, the Ni-PP-based GDE + PE and SS + PP presented slightly better results than NF + PP (Table 1). The Ni-PP-based GDE + PE achieved an average R_{rec} of 5.3 ± 0.4 gN-NH_4^+ d^{-1} m^{-2}, and an E_{rec} of 18.9 ± 4.0 %. Reported rates and efficiencies were calculated as the average of the last three consecutive batches for each condition, during which system performance was stable. For these batches, the NH_4^+ mass balance deviation was always below 13 %. All the alternative strategies allowed higher

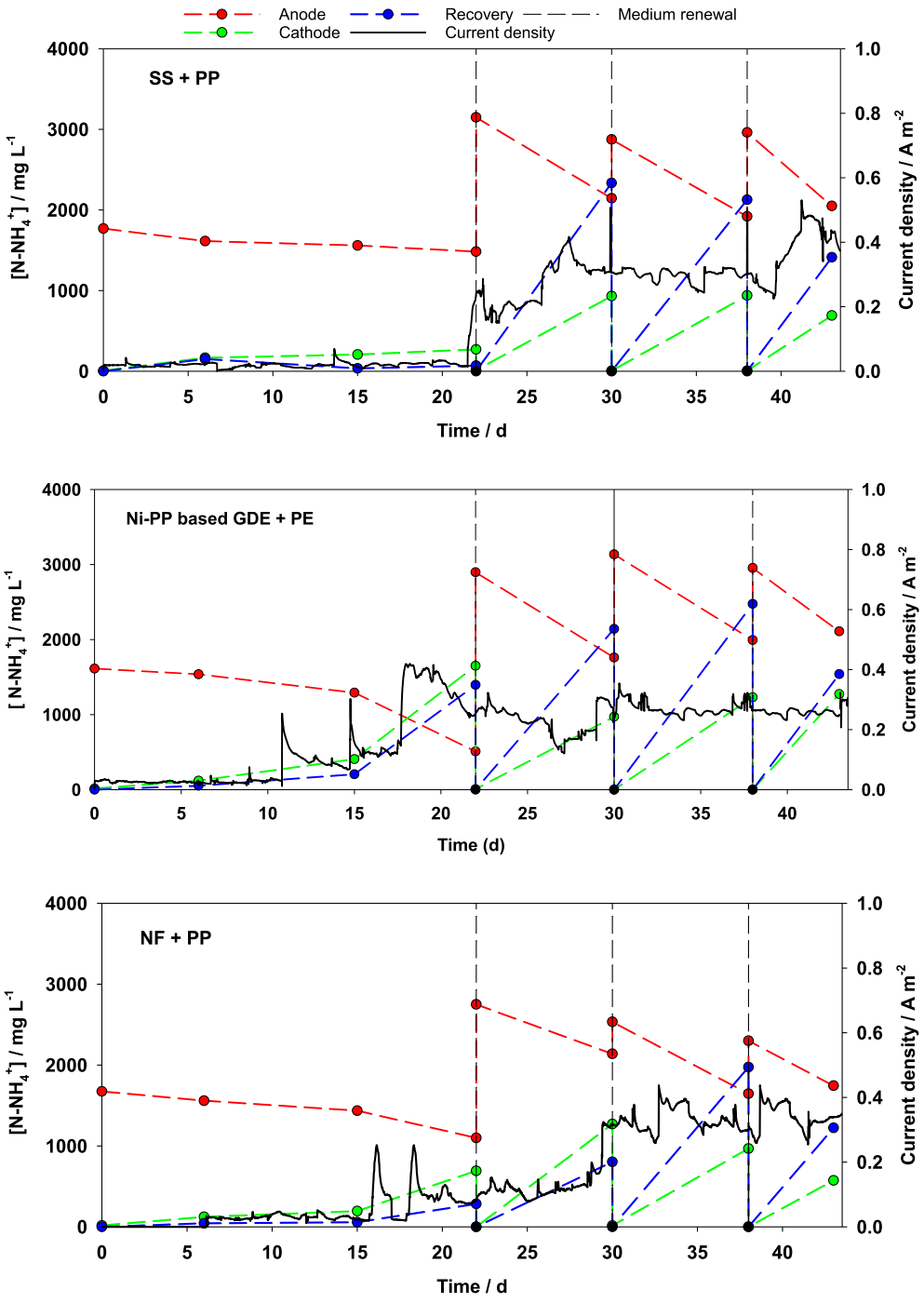

Fig. 5. Current density and concentration of $N\text{-}NH_4^+$ obtained for different cathode approaches.

Table 1
Average current densities, ammonium removal and recovery performance (efficiencies and rates) with different cathodic assemblies. Values represent the average of the last three stable batches. R_{rem} (ammonium removal rate); E_{rem} (ammonium removal efficiency); R_{rec} (ammonium recovery rate); E_{rec} (ammonium recovery efficiency). Experimental error is standard deviation ($n = 2$).

Cathode material	Applied voltage (V)	Average R_{rem} ($gN\text{-}NH_4^+$ m^{-2} d^{-1})	Average E_{rem} (%)	Average R_{rec} ($gN\text{-}NH_4^+$ m^{-2} d^{-1})	Average E_{rec} (%)	Average current density (A m^{-2})
SS + PP	1.2	9.3 ± 2.3	31.9 ± 1.2	5.0 ± 0.2	18.1 ± 4.2	0.31 ± 0.05
NF + PP	1.2	6.5 ± 1.3	27.1 ± 7.0	3.6 ± 1.5	14.8 ± 6.7	0.27 ± 0.12
Ni-PP-based GDE + PE	1.2	9.8 ± 1.0	34.7 ± 5.5	5.3 ± 0.4	18.9 ± 4.0	0.25 ± 0.02

current densities and longer operation times than the original Ni-PP-based GDE, which failed after 14 days. However, the performance was much lower than in the abiotic systems, so it was necessary to look for better-operating conditions to approach the yields obtained abiotically.

3.2.4. Effects of applied voltages

Fig. 6 illustrates the current density obtained for the three cathode materials at different applied voltages. Each batch was initiated with acetate addition, indicated by the dashed lines, and the batch duration was defined based on system performance, with acetate added again when current began to decline. The voltage was maintained for 2 batches and the catholyte and recovery solutions were replenished after each batch. The influence of applied voltage on current density and, consequently, on ammonium recovery was investigated using selected cathodic configurations. After acclimation at 1.2 V, the applied voltage was decreased to 1.0 V and then to 0.8 V. At an applied voltage of 1.0 V, current density with three cathode materials was only slightly decreased and was further decreased when 0.8 V was used. During these cycles, the CE reduced to 14 % (NF + PP), 16 % (Ni-PP-based GDE + PE) and 16 % (SS + PP) for 0.8 V compared to 54 % (NF + PP), 48 % (Ni-PP-based GDE + PE) and 61 % (SS + PP) for 1 V. These results suggest that a low applied voltage affects the bioanode's microbial activity because of the low anode potential.

Expectedly, higher applied voltage led to higher E_{rem} and E_{rec} as well as higher R_{rem} and R_{rec} since higher current densities allow better electron transfer ability. The application of high voltage provided good conditions for the microbial community on the anode.

Although there are limited studies that have investigated the effect of applied voltage on ammonium recovery in BES systems, one such study by Kondaveeti et al. [51] examined ammonia removal in a dual-chamber MEC, via a process described as simultaneous nitrification and denitrification, using applied voltages ranging from 0.7 V to 1.5 V. The proposed mechanism involved oxygen generation via water electrolysis at the anode to support aerobic nitrifiers, followed by autotrophic denitrification at the cathode. Their results demonstrated that increasing the applied voltage enhanced nitrification rates, with total ammonia removal reaching 85 % at 1.5 V. This improvement was attributed to enhanced electron transfer and stimulation of microbial activity, leading to higher nitrification rates. This aligns with the findings in our study, where the applied voltage similarly influenced the efficiency of ammonium recovery, underscoring the importance of voltage in optimizing performance in BES systems.

Following the two cycles at 1.4 V, the applied voltage was restored to 1.0 V. The current density obtained was lower than what was obtained previously with 1.0 V for all the cathode materials tested, indicating that the microbial community was still active even after being exposed to a high applied voltage of 1.4 V but the materials might have been affected. In fact, after several months of operation, the SS sheets used as the current collectors (AISI 316) were observed to suffer from corrosion, which is presumed to result from the anode potential reaching values above the potential at which oxidation of the SS occurs. Electrochemical analysis of the material (CV and CA) indicated that oxidation occurred at potentials above 0.3 V vs Ag/AgCl (Fig. S4). The ammonium removal and recovery exhibited a slightly rising trend with applied voltage (Fig. 7). The lowest R_{rec} was obtained for NF + PP at 0.8 V. The low current density and rates obtained indicated that an applied voltage of 0.8 V was insufficient to recover ammonium. The highest R_{rem} (21 gN-NH_4^+ m^{-2} d^{-1}) was obtained for SS + PP at 1.4 V mainly due to its higher current density, which increased the cation migration. This higher R_{rem} also led to a higher R_{rec} (17 gN-NH_4^+ m^{-2} d^{-1}).

Thus, in order to determine the effect of applying a potential of 1.4 V to the cathode materials, further research is necessary. However, it can be concluded that a voltage of 1.4 V would be appropriate for the biological recovery of ammonium. The difference between R_{rem} and R_{rec} obtained for the cathode materials is quite noticeable (e.g., 19 % for SS + PP at 1.4 V). This indicates that not all ammonium reaching the cathode chamber is recovered, possibly due to incomplete conversion of ammonium to ammonia caused by too low catholyte's pH or to losses through system leakages. To evaluate overall recovery efficiency, ammonium mass balances were performed for each batch by comparing the total NH_4^+ present in all three chambers at the start and at the end of the batch. Deviations were below 15 %, indicating limited losses.

Due to the higher removal and recovery efficiencies, the energy consumed per kg_N removed or recovered remained lower with an applied voltage of 1.4 V than with 1.0 V or 1.2 V, considering only the external energy applied with the power source (Fig. 8). The lowest energy consumption of 0.34 kWh kg_N^{-1} removed was obtained with 0.8 V of applied voltage with Ni-PP based GDE + PE.

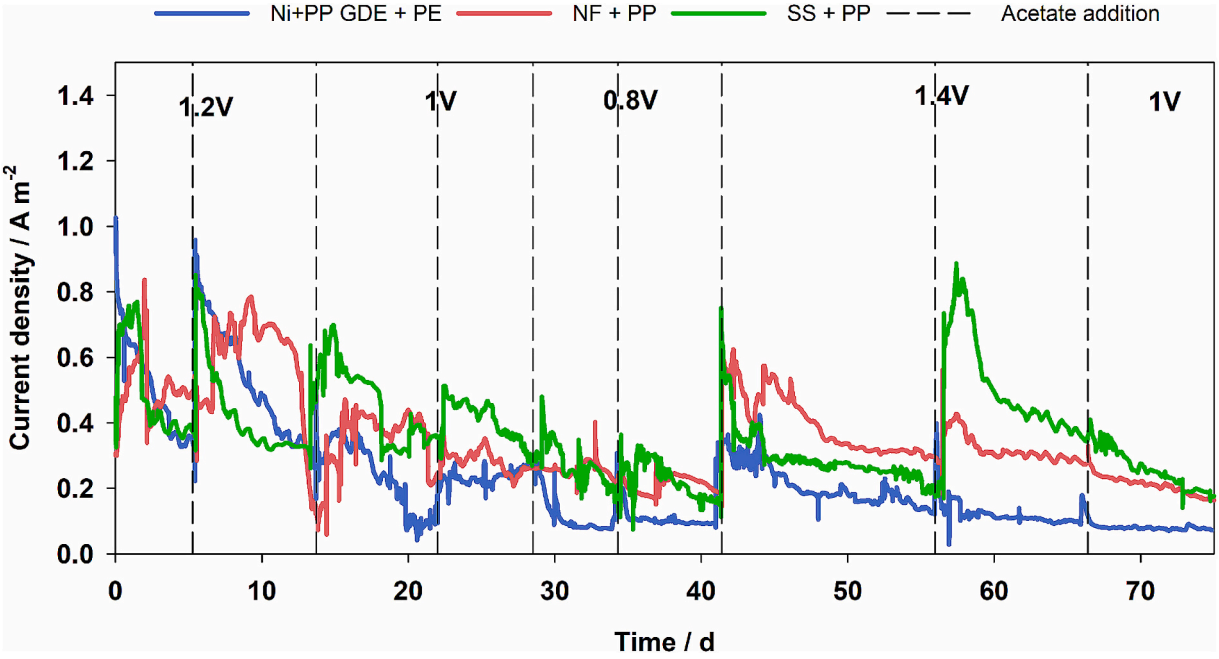

Fig. 6. Current density obtained for different applied voltages. Dashed lines represent acetate dosages.

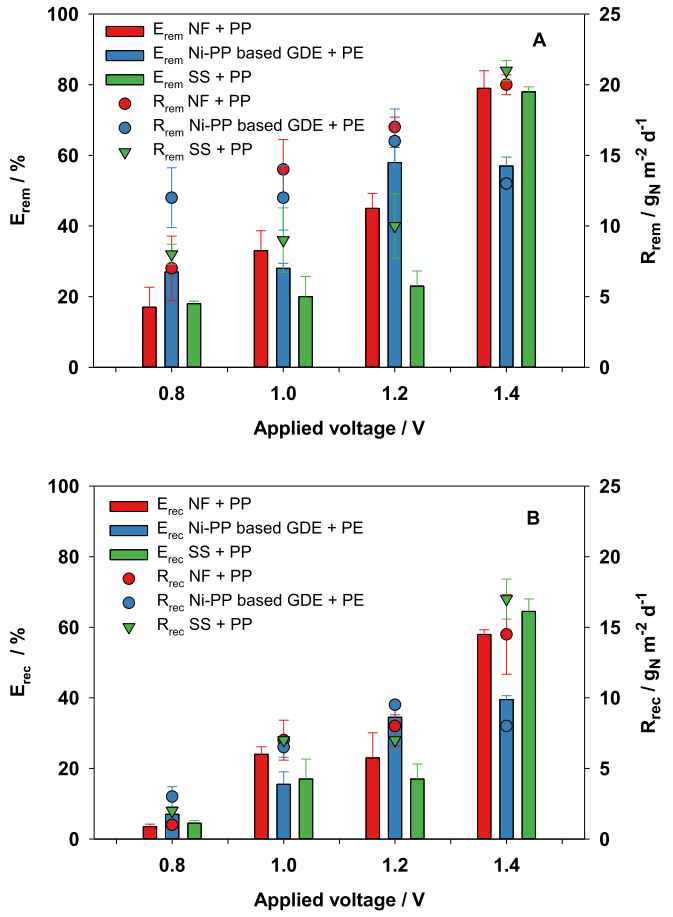

Fig. 7. The effect of applied voltage on the bioelectrochemical ammonium recovery with different cathodic configurations (A) Removal (B) Recovery. Experimental error is standard deviation ($n = 2$).

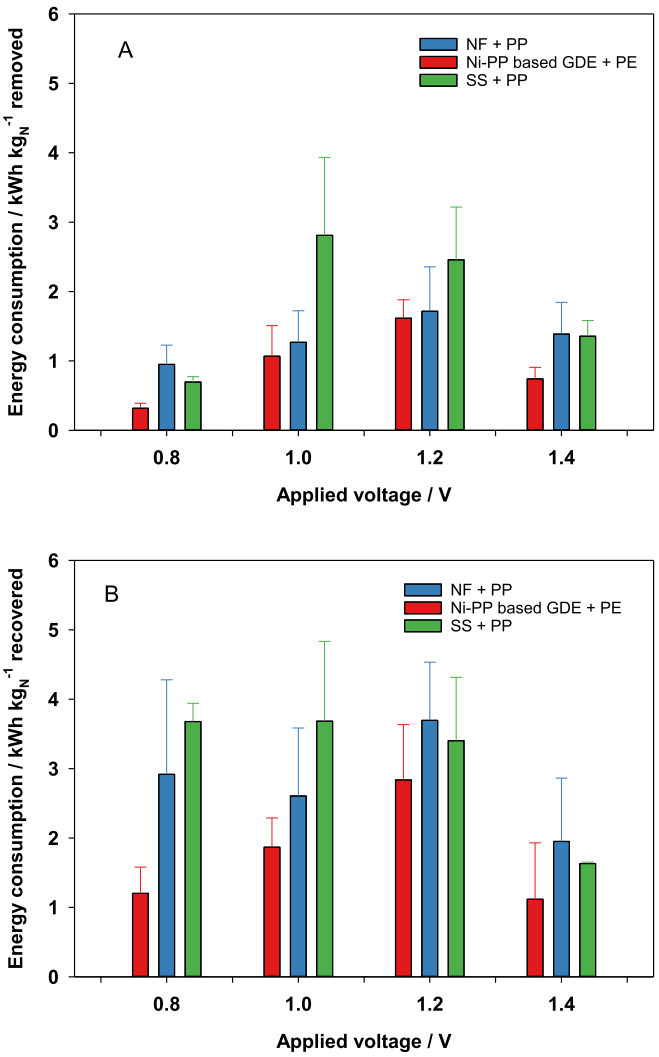

Fig. 8. (A) Energy consumption per N removed. (B) Energy consumption per N recovered. Experimental error is standard deviation (n = 2).

In a nutshell, comparing abiotic and biotic experiments, the current densities obtained in this study for abiotic systems are 7 times higher than those in biotic systems. In abiotic system, the highest recovery rate achieved was 55 gN-NH_4^+ m^{-2} d^{-1} which is almost 3 times higher than the 17 gN-NH_4^+ m^{-2} d^{-1} obtained in the biotic setup. This high recovery rate in the abiotic setup was achieved at expenses of applying a high current of 75 mA, leading to an energy consumption of nearly 16 kWh per kg of nitrogen removed. In contrast, the energy consumption in biotic systems did not exceed 3 kWh per kg of nitrogen removed. While the current generated in the biotic system is lower compared to the abiotic system, the biotic system offers notable benefits. It requires less energy and can harness electrons from wastewater instead of depending on the water oxidation reaction on the anode (i.e. oxygen evolution reaction, OER). In addition, the energy needed to recover each kg of nitrogen is significantly lower in biotic systems (less than 4 kWh kg_N^{-1} recovered) compared to abiotic setups (nearly 26 kWh kg_N^{-1} recovered), which supports the prevailing emphasis on BES.

The energy consumption values observed in our study are competitive when compared to those reported in the literature for TMCS systems utilized for ammonium recovery. Specifically, Hou et al. [19] reported an energy consumption of 1.61 kWh kg_N^{-1} using a Ni-based GDE, achieving a significantly higher nitrogen recovery rate (R_{rec}) of 36.2 gN m^{-2} d^{-1}. However, it is important to note that the duration of their experiments was relatively brief, lasting approximately 13 days, which may not have fully captured the long-term stability and performance of the system. In contrast, Cerrillo et al. [32] reported an energy consumption of 5 kWh kg_N^{-1} and a lower nitrogen recovery rate of 6.72 gN m^{-2} d^{-1}. These variations in results highlight the lack of consensus in the literature regarding energy consumption and recovery rates for TMCS-based ammonium recovery systems. Overall, while the energy consumption in our study aligns with the values reported in the literature, it underscores the potential for further optimization in both nitrogen recovery rates and energy efficiency.

Nevertheless, the decreased current densities in biotic setups lead to a decline in ammonium recovery rates. In order to tackle this issue, future endeavours should focus on enhancing the current densities in BES by optimizing several aspects like electrode materials, biofilm formation, and the organic matter source. In addition, the amount of ammonium in the feed is of utmost importance. The process of ammonium recovery is specifically intended for wastewater that contains high concentrations of NH_4^+. This is because higher concentrations of anolyte (the solution on the anode side of an electrochemical cell) facilitate the transport of NH_4^+ via the CEM. It will be crucial to consider all of these parameters in future studies in order to enhance ammonium recovery in BES.

4. Conclusions

The long-term operation for bioelectrochemical ammonium recovery using a hydrophobic membrane with different cathode materials was demonstrated. The main conclusions of this research work are summarized below:

- It was possible to operate the electrochemical system at an intensity of 50 mA. Even though the maximum recovery rate (55 gN-NH_4^+ m^{-2} d^{-1}) is higher with 75 mA, severe damage was observed to GDE.
- Regarding cation migration through the CEM, a higher ammonium concentration in the anolyte favours the selective electromigration of ammonium from the anolyte.
- When working with only Ni-PP-based GDE, the degradation of the electrode was observed after a short period of operation.
- Of the tested alternatives, the best results were obtained with SS achieving a maximum removal rate of 21 gN-NH_4^+ m^{-2} d^{-1} at 1.4 V because of higher current density, leading to increased cation migration.
- Higher removal and recovery efficiencies allowed for lower energy consumption per g_N removed/recovered at an applied voltage of 1.4 V than at 1.0 V or 1.2 V.

CRediT authorship contribution statement

Zainab Ul: Writing – review & editing, Writing – original draft, Visualization, Methodology, Investigation, Formal analysis, Data curation, Conceptualization. **Mariella Belén Galeano:** Visualization, Methodology, Investigation. **Mira Sulonen:** Writing – review & editing, Supervision, Methodology, Investigation, Formal analysis, Data curation, Conceptualization. **Mireia Baeza:** Writing – review & editing, Software, Methodology, Formal analysis, Data curation, Conceptualization. **Juan Antonio Baeza:** Writing – review & editing, Visualization, Validation, Supervision, Software, Methodology, Formal analysis, Data curation, Conceptualization. **Albert Guisasola:** Writing – review & editing, Visualization, Validation, Supervision, Resources, Project administration, Methodology, Funding acquisition, Formal analysis, Data curation, Conceptualization.

Declaration of competing interest

The authors declare that they have no known competing financial interests or personal relationships that could have appeared to influence the work reported in this paper.

Acknowledgements

The authors acknowledge the support of the VIVALDI project that has received funding from the European Union's Horizon 2020 research and innovation programme under grant agreement 101000441. The authors are members of the GENOCOV research group (Grup de Recerca Consolidat de la Generalitat de Catalunya, 2021 SGR 515, www.genocov.com). Albert Guisasola acknowledges the funding from the ICREA Academia grant.

Appendix A. Supplementary data

Supplementary data to this article can be found online at https://doi.org/10.1016/j.bioelechem.2025.109013.

Data availability

Data will be made available on request.

References

[1] D. Puyol, D.J. Batstone, T. Hülsen, S. Astals, M. Peces, J.O. Krömer, Resource recovery from wastewater by biological technologies: opportunities, challenges, and prospects, Front. Microbiol. 7 (2017), https://doi.org/10.3389/fmicb.2016.02106.
[2] P.T. Kelly, Z. He, Nutrients removal and recovery in bioelectrochemical systems: a review, Bioresour. Technol. 153 (2014) 351–360, https://doi.org/10.1016/j.biortech.2013.12.046.
[3] Y.V. Nancharaiah, S. Venkata Mohan, P.N.L. Lens, Recent advances in nutrient removal and recovery in biological and bioelectrochemical systems, Bioresour. Technol. 215 (2016) 173–185, https://doi.org/10.1016/j.biortech.2016.03.129.
[4] M. Wang, M.A. Khan, I. Mohsin, J. Wicks, A.H. Ip, K.Z. Sumon, C.-T. Dinh, E. H. Sargent, I.D. Gates, M.G. Kibria, Can sustainable ammonia synthesis pathways compete with fossil-fuel based Haber–Bosch processes? Energy Environ. Sci. 14 (2021) 2535–2548, https://doi.org/10.1039/D0EE03808C.
[5] M. Rodríguez Arredondo, P. Kuntke, A.W. Jeremiasse, T.H.J.A. Sleutels, C.J. N. Buisman, A. ter Heijne, Bioelectrochemical systems for nitrogen removal and recovery from wastewater, Environ. Sci.: Water Res. Technol. 1 (2015) 22–33, https://doi.org/10.1039/C4EW00066H.
[6] S. Georg, C. Schott, J.R. Courela Capitao, T. Sleutels, P. Kuntke, A. ter Heijne, C.J. N. Buisman, Bio-electrochemical degradability of prospective wastewaters to determine their ammonium recovery potential, Sustain. Energy Technol. Assess 47 (2021) 101423, https://doi.org/10.1016/j.seta.2021.101423.
[7] J.W. Erisman, M.A. Sutton, J. Galloway, Z. Klimont, W. Winiwarter, How a century of ammonia synthesis changed the world, Nat. Geosci. 1 (2008) 636–639, https://doi.org/10.1038/ngeo325.
[8] O. Herbinet, P. Bartocci, A. Grinberg Dana, On the use of ammonia as a fuel – a perspective, Fuel Commun. 11 (2022) 100064, https://doi.org/10.1016/j.jfueco.2022.100064.
[9] M.B. Galeano, M. Sulonen, Z. Ul, M. Baeza, J.A. Baeza, A. Guisasola, Bioelectrochemical ammonium recovery from wastewater: a review, Chem. Eng. J. 472 (2023) 144855, https://doi.org/10.1016/j.cej.2023.144855.
[10] Z. Ul, P. Sánchez-Peña, M. Baeza, M. Sulonen, D. Gabriel, J.A. Baeza, A. Guisasola, Systematic screening of carbon-based anode materials for bioelectrochemical systems, J. Chem. Technol. Biotechnol. 98 (2023) 1402–1415, https://doi.org/10.1002/jctb.7357.
[11] C. Santoro, C. Arbizzani, B. Erable, I. Ieropoulos, Microbial fuel cells: from fundamentals to applications. A review, J. Power Sources 356 (2017) 225–244, https://doi.org/10.1016/j.jpowsour.2017.03.109.
[12] A. Kadier, Y. Simayi, P. Abdeshahian, N.F. Azman, K. Chandrasekhar, M.S. Kalil, A comprehensive review of microbial electrolysis cells (MEC) reactor designs and configurations for sustainable hydrogen gas production, Alex. Eng. J. 55 (2016) 427–443, https://doi.org/10.1016/j.aej.2015.10.008.
[13] S. Kondaveeti, J. Lee, R. Kakarla, H.S. Kim, B. Min, Low-cost separators for enhanced power production and field application of microbial fuel cells (MFCs), Electrochim. Acta 132 (2014) 434–440, https://doi.org/10.1016/j.electacta.2014.03.046.
[14] K. Yang, M. Qin, The application of cation exchange membranes in electrochemical Systems for Ammonia Recovery from wastewater, Membranes 11 (2021) 494, https://doi.org/10.3390/membranes11070494.
[15] H. Wang, Z.J. Ren, A comprehensive review of microbial electrochemical systems as a platform technology, Biotechnol. Adv. 31 (2013) 1796–1807, https://doi.org/10.1016/j.biotechadv.2013.10.001.
[16] P. Zamora, T. Georgieva, A. Ter Heijne, T.H.J.A. Sleutels, A.W. Jeremiasse, M. Saakes, C.J.N. Buisman, P. Kuntke, Ammonia recovery from urine in a scaled-up microbial electrolysis cell, J. Power Sources 356 (2017) 491–499, https://doi.org/10.1016/j.jpowsour.2017.02.089.
[17] X. Wu, O. Modin, Ammonium recovery from reject water combined with hydrogen production in a bioelectrochemical reactor, Bioresour. Technol. 146 (2013) 530–536, https://doi.org/10.1016/j.biortech.2013.07.130.
[18] K.Y. Cheng, A.H. Kaksonen, R. Cord-Ruwisch, Ammonia recycling enables sustainable operation of bioelectrochemical systems, Bioresour. Technol. 143 (2013) 25–31, https://doi.org/10.1016/j.biortech.2013.05.108.
[19] D. Hou, A. Iddya, X. Chen, M. Wang, W. Zhang, Y. Ding, D. Jassby, Z.J. Ren, Nickel-based membrane electrodes enable high-rate electrochemical Ammonia recovery, Environ. Sci. Technol. 52 (2018) 8930–8938, https://doi.org/10.1021/acs.est.8b01349.
[20] Z. Ul, M. Sulonen, J.A. Baeza, A. Guisasola, Continuous high-purity bioelectrochemical nitrogen recovery from high N-loaded wastewaters, Bioelectrochemistry 158 (2024) 108707, https://doi.org/10.1016/j.bioelechem.2024.108707.
[21] M. Cerrillo, L. Burgos, E. Serrano-Finetti, V. Riau, J. Noguerol, A. Bonmatí, Hydrophobic membranes for ammonia recovery from digestates in microbial electrolysis cells: assessment of different configurations, J. Environ. Chem. Eng. 9 (2021) 105289, https://doi.org/10.1016/j.jece.2021.105289.
[22] M. Maurer, P. Schwegler, T.A. Larsen, Nutrients in urine: energetic aspects of removal and recovery, Water Sci. Technol. 48 (2003) 37–46, https://doi.org/10.2166/wst.2003.0011.
[23] M. Maurer, W. Pronk, T.A. Larsen, Treatment processes for source-separated urine, Water Res. 40 (2006) 3151–3166, https://doi.org/10.1016/j.watres.2006.07.012.
[24] S.K. Pradhan, A. Mikola, R. Vahala, Nitrogen and phosphorus harvesting from human urine using a stripping, absorption, and precipitation process, Environ. Sci. Technol. 51 (2017) 5165–5171, https://doi.org/10.1021/acs.est.6b05402.
[25] J. Desloover, A. Abate Woldeyohannis, W. Verstraete, N. Boon, K. Rabaey, Electrochemical resource recovery from Digestate to prevent Ammonia toxicity during anaerobic digestion, Environ. Sci. Technol. 46 (2012) 12209–12216, https://doi.org/10.1021/es3028154.
[26] S. Gildemyn, A.K. Luther, S.J. Andersen, J. Desloover, K. Rabaey, Electrochemically and bioelectrochemically induced ammonium recovery, JoVE (2015) 52405, https://doi.org/10.3791/52405.
[27] P. Kuntke, K.M. Śmiech, H. Bruning, G. Zeeman, M. Saakes, T.H.J.A. Sleutels, H.V. M. Hamelers, C.J.N. Buisman, Ammonium recovery and energy production from urine by a microbial fuel cell, Water Res. 46 (2012) 2627–2636, https://doi.org/10.1016/j.watres.2012.02.025.

[28] Y. Liu, M. Qin, S. Luo, Z. He, R. Qiao, Understanding ammonium transport in bioelectrochemical systems towards its recovery, Sci. Rep. 6 (2016) 22547, https://doi.org/10.1038/srep22547.
[29] P. Kuntke, P. Zamora, M. Saakes, C.J.N. Buisman, H.V.M. Hamelers, Gas-permeable hydrophobic tubular membranes for ammonia recovery in bio-electrochemical systems, Environ. Sci.: Water Res. Technol. 2 (2016) 261–265, https://doi.org/10.1039/C5EW00299K.
[30] M.E.R. Christiaens, K.M. Udert, J.B.A. Arends, S. Huysman, L. Vanhaecke, E. McAdam, K. Rabaey, Membrane stripping enables effective electrochemical ammonia recovery from urine while retaining microorganisms and micropollutants, Water Res. 150 (2019) 349–357, https://doi.org/10.1016/j.watres.2018.11.072.
[31] C. Gao, L. Liu, T. Yu, F. Yang, Development of a novel carbon-based conductive membrane with in-situ formed MnO2 catalyst for wastewater treatment in bio-electrochemical system (BES), J. Membr. Sci. 549 (2018) 533–542, https://doi.org/10.1016/j.memsci.2017.12.053.
[32] M. Cerrillo, L. Burgos, A. Bonmatí, Biogas upgrading and Ammonia recovery from livestock manure Digestates in a combined Electromethanogenic biocathode—hydrophobic membrane system, Energies 14 (2021) 503, https://doi.org/10.3390/en14020503.
[33] P. Kuntke, T.H.J.A. Sleutels, M. Rodríguez Arredondo, S. Georg, S.G. Barbosa, A. Ter Heijne, H.V.M. Hamelers, C.J.N. Buisman, (Bio)electrochemical ammonia recovery: progress and perspectives, Appl. Microbiol. Biotechnol. 102 (2018) 3865–3878, https://doi.org/10.1007/s00253-018-8888-6.
[34] W.A. Tarpeh, J.M. Barazesh, T.Y. Cath, K.L. Nelson, Electrochemical stripping to recover nitrogen from source-separated urine, Environ. Sci. Technol. 52 (2018) 1453–1460, https://doi.org/10.1021/acs.est.7b05488.
[35] S. Georg, A.T. Puari, M.P.G. Hanantyo, T. Sleutels, P. Kuntke, A. ter Heijne, C.J. N. Buisman, Low-energy ammonium recovery by a combined bio-electrochemical and electrochemical system, Chem. Eng. J. 454 (2023) 140196, https://doi.org/10.1016/j.cej.2022.140196.
[36] M. Oliot, S. Galier, H. Roux de Balmann, A. Bergel, Ion transport in microbial fuel cells: key roles, theory and critical review, Appl. Energy 183 (2016) 1682–1704, https://doi.org/10.1016/j.apenergy.2016.09.043.
[37] P. Kuntke, M. Geleji, H. Bruning, G. Zeeman, H.V.M. Hamelers, C.J.N. Buisman, Effects of ammonium concentration and charge exchange on ammonium recovery from high strength wastewater using a microbial fuel cell, Bioresour. Technol. 102 (2011) 4376–4382, https://doi.org/10.1016/j.biortech.2010.12.085.
[38] J.A. Baeza, À. Martínez-Miró, J. Guerrero, Y. Ruiz, A. Guisasola, Bioelectrochemical hydrogen production from urban wastewater on a pilot scale, J. Power Sources 356 (2017) 500–509, https://doi.org/10.1016/j.jpowsour.2017.02.087.
[39] J. Ortiz, E. Exposito, F. Gallud, V. Garciagarcia, V. Montiel, A. Aldaz, Desalination of underground brackish waters using an electrodialysis system powered directly by photovoltaic energy, Sol. Energy Mater. Sol. Cells 92 (2008) 1677–1688, https://doi.org/10.1016/j.solmat.2008.07.020.
[40] A. Sotres, M. Cerrillo, M. Viñas, A. Bonmatí, Nitrogen recovery from pig slurry in a two-chambered bioelectrochemical system, Bioresour. Technol. 194 (2015) 373–382, https://doi.org/10.1016/j.biortech.2015.07.036.
[41] K. Yang, M. Qin, Enhancing selective ammonium transport in membrane electrochemical systems, Water Res. 257 (2024) 121668, https://doi.org/10.1016/j.watres.2024.121668.
[42] D. Losantos, M. Aliaguilla, D. Molognoni, M. González, P. Bosch-Jimenez, S. Sanchis, A. Guisasola, E. Borràs, Development and optimization of a bioelectrochemical system for ammonium recovery from wastewater as fertilizer, Clean. Engi. Technol. 4 (2021) 100142, https://doi.org/10.1016/j.clet.2021.100142.
[43] M. Rodríguez Arredondo, P. Kuntke, A. ter Heijne, H.V.M. Hamelers, C.J. N. Buisman, Load ratio determines the ammonia recovery and energy input of an electrochemical system, Water Res. 111 (2017) 330–337, https://doi.org/10.1016/j.watres.2016.12.051.
[44] A. Iddya, D. Hou, C.M. Khor, Z. Ren, J. Tester, R. Posmanik, A. Gross, D. Jassby, Efficient ammonia recovery from wastewater using electrically conducting gas stripping membranes, environ, Sci.: Nano 7 (2020) 1759–1771, https://doi.org/10.1039/C9EN01303B.
[45] A. Kundu, J.N. Sahu, G. Redzwan, M.A. Hashim, An overview of cathode material and catalysts suitable for generating hydrogen in microbial electrolysis cell, Int. J. Hydrog. Energy 38 (2013) 1745–1757, https://doi.org/10.1016/j.ijhydene.2012.11.031.
[46] L. Gil-Carrera, P. Mehta, A. Escapa, A. Morán, V. García, S.R. Guiot, B. Tartakovsky, Optimizing the electrode size and arrangement in a microbial electrolysis cell, Bioresour. Technol. 102 (2011) 9593–9598, https://doi.org/10.1016/j.biortech.2011.08.026.
[47] X. Hu, X. Tian, Y.-W. Lin, Z. Wang, Nickel foam and stainless steel mesh as electrocatalysts for hydrogen evolution reaction, oxygen evolution reaction and overall water splitting in alkaline media, RSC Adv. 9 (2019) 31563–31571, https://doi.org/10.1039/C9RA07258F.
[48] O. Guerrero-Sodric, J.A. Baeza, A. Guisasola, Enhancing bioelectrochemical hydrogen production from industrial wastewater using Ni-foam cathodes in a microbial electrolysis cell pilot plant, Water Res. 256 (2024) 121616, https://doi.org/10.1016/j.watres.2024.121616.
[49] M. Shalom, D. Ressnig, X. Yang, G. Clavel, T.P. Fellinger, M. Antonietti, Nickel nitride as an efficient electrocatalyst for water splitting, J. Mater. Chem. A 3 (2015) 8171–8177, https://doi.org/10.1039/C5TA00078E.
[50] R. Subbaraman, D. Tripkovic, D. Strmcnik, K.-C. Chang, M. Uchimura, A. P. Paulikas, V. Stamenkovic, N.M. Markovic, Enhancing hydrogen evolution activity in water splitting by tailoring Li^+-$Ni(OH)_2$-Pt interfaces, Science 334 (2011) 1256–1260, https://doi.org/10.1126/science.1211934.
[51] S. Kondaveeti, D.-H. Choi, M.T. Noori, B. Min, Ammonia removal by simultaneous nitrification and denitrification in a single dual-chamber microbial electrolysis cell, Energies 15 (2022) 9171, https://doi.org/10.3390/en15239171.